Available online at www.sciencedirect.com
SCIENCE DIRECT®
Journal of Power Sources 124 (2003) 271–277
JOURNAL OF POWER SOURCES
www.elsevier.com/locate/jpowsour

Studies of current and potential distributions on lead-acid batteries I. Discharge of automotive flooded positive plates

Yonglang Guo [a,*], Yi Li [a], Guodong Zhang [a], Huiming Zhang [b], J. Garche [c]

[a] *Department of Chemistry, Shandong University, Jinan 250100, PR China*
[b] *Jin Fengfan Storage Battery Co. Ltd., Baoding 071057, PR China*
[c] *Center for Solar Energy and Hydrogen Research, D-89081 Ulm, Germany*

Received 4 February 2003; accepted 30 June 2003

Abstract

The distributions of current and potential on the automotive positive plate have been studied. In the early stage of the discharge, the distributions of the current density, potential, and polarization resistance are uniform. In the later stage, however, the polarization resistance of the active mass increases very rapidly at the bottom and on the top of the plate. It causes the polarization to become very high and makes the current drop rapidly in these regions. It is also found that at the beginning of the 3 C discharge, the higher current density appears in the lower part rather than in the upper part of the plate, which is different from the conventional viewpoint. This may be due to the improper formation and overcharge of the plate.

Keywords: Automotive battery; Distribution of current and potential; Lead-acid battery; Positive plate

1. Introduction

Over the decade, R&D has focused on the valve-regulated lead-acid batteries, not on flooded lead-acid batteries. Up to now the flood lead-acid batteries are primarily used for automotive starting–lighting–ignition (SLI). It is well known that except for the cold-cranking ability (CCA), the performance of the automotive batteries is mainly limited by the positive plate such as grid corrosion and the softening of the active mass, etc. [1–4]. The research work of the positive plate involves mainly the plate manufacture and the grid design. The grid design work is often connected with the grid resistance simulation to minimize resistance losses [5–8]. The use of anti-corroded alloys for the grid causes the plate to be thinner, which has reduced the weight and has greatly improved the starting performance of the automotive battery [9]. On the other hand, the manufacturing technology of the positive plate has also been widely studied. Involved have been the lead paste production parameters, such as the content of the oxide, H_2SO_4, water, and the additive and the density of the paste [10,11]. A proper curing process improves both the initial structure of the active mass and the interface between the grid and the active mass and therefore the life of the battery [12]. In order to ensure the dry-charged performance of the automotive battery, it is necessary to boost the electrolyte temperature properly or/and use multi-step current in the formation of the plate, to increase the content of PbO_2 in the positive active mass [13–16].

Since the positive potential drops more quickly than the negative potential during the discharge of the battery (except the discharge at low temperature), the study so far has concentrated more on the positive grid design optimizing, the simulated tests and calculation of the current and potential distributions of positive plates [17,18]. There is only little work on the practical measurement of the current and potential distributions [19,20]. In this paper, these distributions have been tested on the surface of the positive plate of automotive flooded batteries. It is shown that there exists great discrepancy between the simulated test or predicted work and the practical results of the measurements.

2. Experimental

The testing plate was a commercial automotive positive plate produced by Jin Fengfan Storage Battery Co. Ltd. The grid used was the conventional orthogonal design and was shown in Fig. 1. It had a dimension of 14.3 cm (W) × 12.5 cm (H) × 0.16 cm (T). The thickness of

* Corresponding author.
E-mail address: yguo@sdu.edu.cn (Y. Guo).

0378-7753/$ – see front matter © 2003 Elsevier B.V. All rights reserved.
doi:10.1016/S0378-7753(03)00768-7

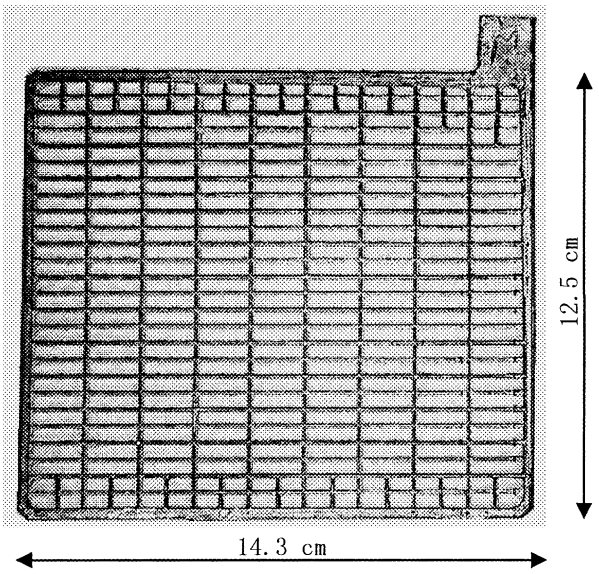

Fig. 1. Picture of automotive positive grid.

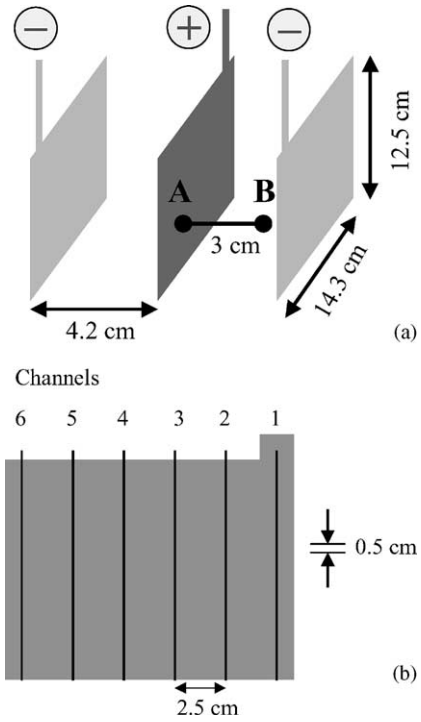

Fig. 2. An experimental scheme. (a) Installation of plates; (b) locations of measurement points.

the pasted positive plate was 0.2 cm. There was about 122 g active mass on each plate, which had a capacity of 12 Ah at the 20 h discharge.

The container used in the experiments had an internal dimension of 14.5 cm (W) × 9.0 cm (L) × 15 cm (H). The width of the container and the height of the H_2SO_4 electrolyte were the same as the dimensions of the positive plate, to ensure the ion flowing between negative and positive plates, which was parallel to each other. Fig. 2a shows the installation of the plates, in which one positive plate was placed between two negative plates. The distance between the positive and negative plates was about 4.2 cm, not typically for practical batteries but this had allowed the reference electrodes to be placed between the plates. That is because the local current density on the surface of the positive plate was measured via the IR voltage drop between points A and B in the H_2SO_4 electrolyte through a couple of $Hg/Hg_2SO_4/H_2SO_4$ (1.285 specific gravity) reference electrodes. The distance between points A and B, perpendicular to the plates, was 3 cm and the outside diameter of the reference electrode tip was about 0.15–0.2 cm. The potential reported in this paper was measured against the reference electrode above. The IR voltage drop and the electrode potentials were recorded by a HP 34970A Data Acquisition/Switch Unit connected to a PC computer. The experiments were conducted at room temperature ($18 \pm 2\,^{\circ}C$).

The locations of measurement points on the positive plate are shown in Fig. 2b. We measured the IR drop with equi-interval from the bottom to the top of the positive plate (every 0.5 cm in height). When three couples of reference electrodes with 2.5 cm in spacing were moved from the bottom to the top twice, we could acquire 156 potential differences and 156 electrode potentials on the surface of the positive plate. The scan time of the reference electrode was 40 s from the bottom to the top. During one discharge, only the data of 78 points were obtained. The other half data were measured again after the positive plate was fully recharged. Therefore, from two scans, we could get the current and potential distributions of six channels on the surface of the automotive positive plate.

The dry-charged positive plate was discharged at 36 A after it was immersed into the H_2SO_4 solution for 20 min at room temperature. In the charge of the positive plate, the overcharge was always performed for 4–5 h at a constant voltage of 2.50 V. Then the wet-charged plate was discharged at 36 A (3 C rate) or 7.5 A (0.625 C rate).

3. Results and discussion

3.1. Resistance distribution of grid

In order to obtain the resistance distribution of the automotive positive grid, we caused the current of 1 A to flow through the grid lug and another point on the grid and accurately measured the voltage drop between these two points. Fig. 3 shows the resistance distribution of the positive grid. It is found that the resistance becomes higher and higher with the increase of the distance away from the grid lug. The greatest resistance occurs in the diagonal region of the lug. However, the resistance around the grid frame becomes small. This is because the big frame increases the conductivity. The highest resistance is only about 4 mΩ.

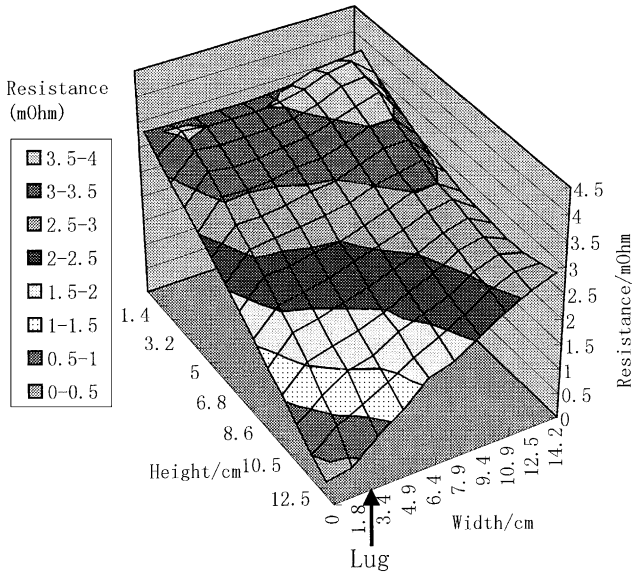

Fig. 3. The resistance distribution of the grid in Fig. 1.

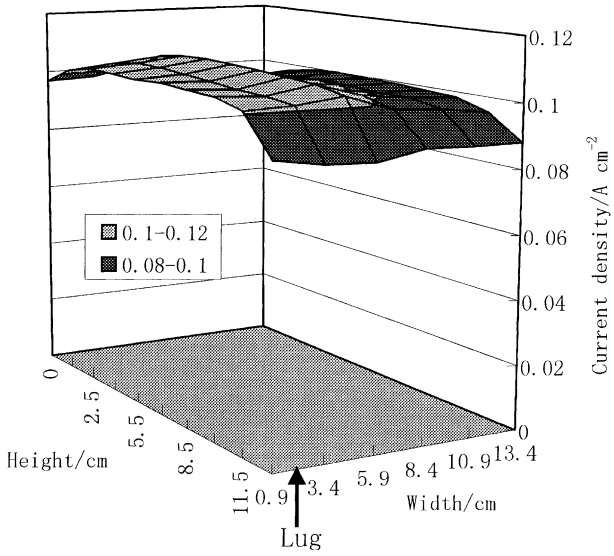

Fig. 4. The distribution of current density on automotive positive plate during discharge of 36 A (3 C rate). Discharge time: 1 min.

3.2. Distributions of current density and potential at high discharge rate (3 C)

Since the electrolyte is excessive under the experiment conditions, the H_2SO_4 concentration changes little during the discharge of the positive plate and so does the electrolyte resistance. In order to obtain the current density distribution on the positive plate, we assume that the electrolyte resistance up and down the battery is uniform during the scan of the reference electrodes from the bottom to top of the positive plate. So the IR drop between points A and B in Fig. 2a is proportional to the current flowing through the electrolyte and the sum of the IR drop with 156 data obtained in two scans is proportional to the current flowing on each side of the plate. Therefore, the current density at any point on the plate can be calculated on the basis of the discharge current, the area of the plate and each IR drop in the electrolyte. When the automotive positive plate was discharged at 36 A (3 C rate), the current at each side of the plate was 18 A. At this time, the current density through points A and B in Fig. 2a can be expressed by

$$i_k = \frac{18 I_k}{1.146 \sum_k I_k} \quad (1)$$

where I_k is the current intensity in the area of 1.146 cm^2 on the positive plate and i_k denotes the current density at this point.

Since great changes took place in the positive potential in the early stage of the discharge at the high discharge rate, the distributions of the current density and the potential were measured on the surface of the automotive positive plate after the discharge of 1 min. As shown in Figs. 4 and 5, respectively, the distribution of the current density is uniform for the most parts of the surface of the positive plate, except for the bottom and the top where a little lower current density appears. The similar phenomenon is observed in the potential distribution of Fig. 5. The higher polarization occurs at the bottom and on the top of the positive plate. As the positive plate was discharged, the distributions of the current density and the potential were measured after a discharge time of 4 and 5.8 min, respectively. It is obvious that the discharge time of this positive plate is much longer than that of the practical automotive batteries. This is because there is too much electrolyte under the experiment conditions. Therefore, the complete discharge leads to a H_2SO_4 concentration decrease of only about 1%. Figs. 6 and 7 show the distributions of the current density and potential at the

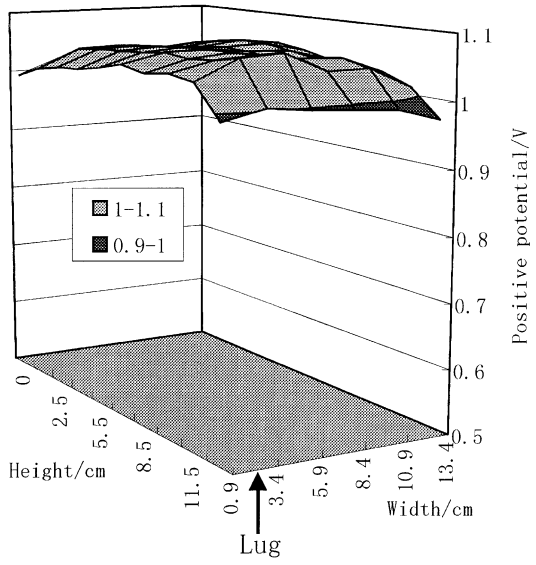

Fig. 5. The potential distribution on automotive positive plate during discharge of 36 A (3 C rate). Discharge time: 1 min.

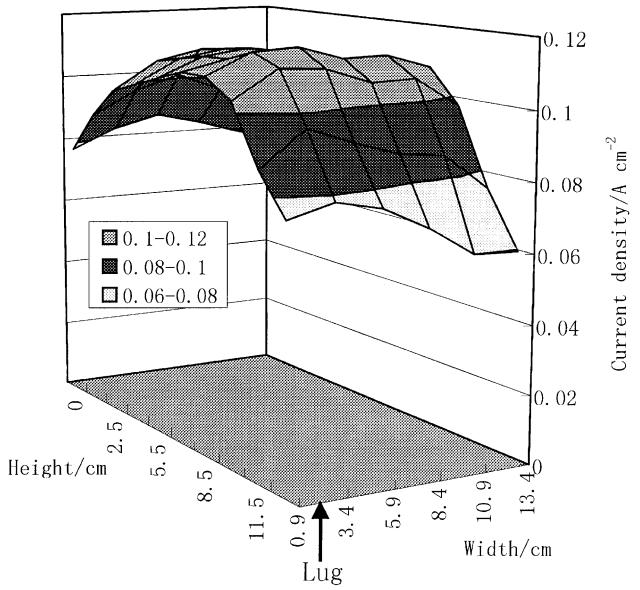

Fig. 6. The distribution of current density on automotive positive plate during discharge of 36 A (3 C rate). Discharge time: 5.8 min.

end of the discharge. At this time, the current density decreases at the bottom and especially on the top, while it increases in the middle of the plate. It is clear that the utilization of the active mass in the middle is higher than that at the bottom and on the top. At the end of the discharge, Fig. 7 shows that the positive potential drops quickly on the whole plate and its distribution is quite non-uniform. The potential at the bottom and on the top becomes very low. The highest polarization occurs on the top of the plate. The quick drop of the potential in these regions will result in the end of the discharge.

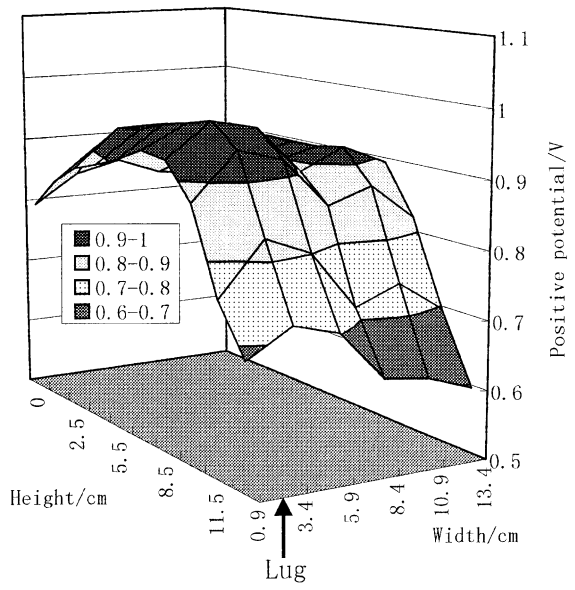

Fig. 7. The potential distribution on automotive positive plate during discharge of 36 A (3 C rate). Discharge time: 5.8 min.

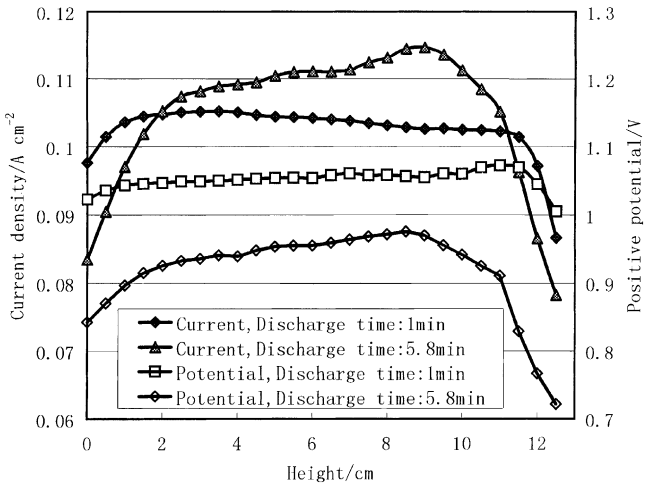

Fig. 8. The distribution of the current density and positive potential in channel 2 at different discharge times. Discharge current: 36 A.

Fig. 8 shows the distribution of the current density and positive potential in channel 2 in Fig. 2b. Although the positive plate is discharged at 36 A (3 C rate), the voltage drop up and down the plate is less than 30 mV after a discharge time of 1 min. It implies that the conductivity of the grid is not a main factor in limiting the discharge of the positive plate and the utilization of the positive active mass. Fig. 8 also shows that the active mass located on the top of the plate limits the discharge of the plate.

It is normally believed that the active mass near the lug or on the top is discharged earlier than that in the lower parts of the plate. But Fig. 8 shows that the current density in the lower part is higher than that in the upper part of the plate, except at the bottom and on the top, when the plate is discharged for 1 min. It indicates that low polarization occurs in the lower part while high polarization appears in the upper part. Since more active mass in the lower part is discharged during the initial period, the current in the upper part is higher than that in the lower part at the end of the discharge (Fig. 8).

3.3. Distributions of current density and potential at medium discharge rate (0.625 C)

Fig. 9 shows the dependence of the positive potential on the height of the automotive plate at different times at the medium discharge rate (0.625 C). It is found that the distribution of the potential is uniform up and down the plate in the initial period of the discharge and it becomes non-uniform only near the end of the discharge. The highest polarization still appears at the bottom and on the top of the plate. Fig. 10 shows the current density distribution of the positive plate after different discharge times. The change in the current density at the beginning of the discharge is similar to that in Fig. 8. The current density in the lower part is higher than that in the upper part of the plate. The position of the current maximum shifts towards the upper part of the

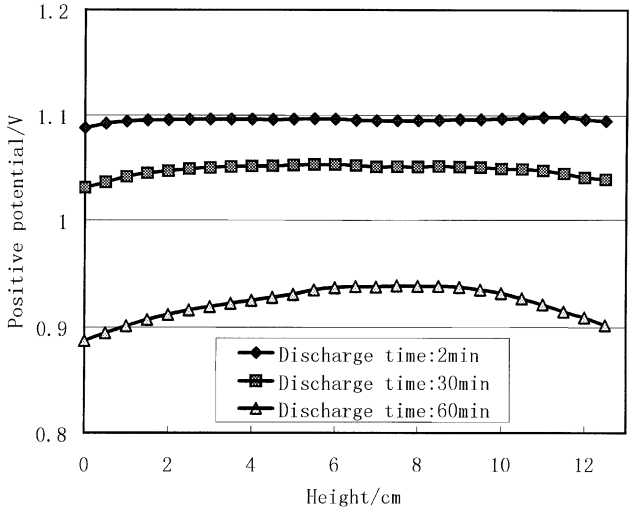

Fig. 9. The positive potential vs. height of the automotive plate in channel 2 during discharge of 7.5 A (0.625 C rate).

plate, while the current at the bottom and on the top always decreases gradually with the discharge. It is clear that more active mass is utilized in the middle part of the plate than at the bottom and on the top.

3.4. Resistance distribution at high discharge rate (3 C)

In order to analyze the polarization at the bottom and on the top of the plate at discharge rates of 3 C (Figs. 5 and 7), the open circuit potential of the fully charged positive plate was measured and it was 1.156 V. When a positive plate is discharged, the polarization resistance can be defined by the ratio of the electrode polarization to the current density. The polarization is mainly caused by the concentration difference, the charge transfer and the resistance of the grid and active mass. Therefore, the potential at any point on the positive plate, U, can be expressed by

$$U = U_0 - \eta_{\text{conc}} - \eta_{\text{ct}} - iR_{\text{grid}} - iR_{\text{grid/AM}} - iR_{\text{AM}} \quad (2)$$

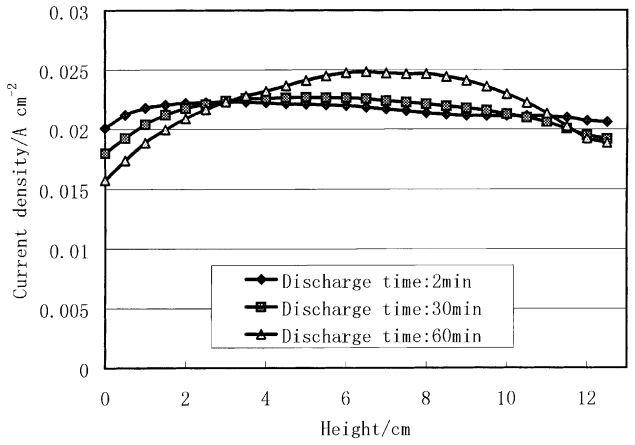

Fig. 10. The current density vs. height of the automotive plate in channel 2 during discharge of 7.5 A (0.625 C rate).

and then during the discharge, the increment of its polarization is equal to

$$-\Delta U = \Delta\eta_{\text{conc}} + \Delta\eta_{\text{ct}} + i(R_{\text{grid}} + R_{\text{grid/AM}} + R_{\text{AM}}) \quad (3)$$

where U_0 denotes the open circuit potential, i the current density at this point, η_{conc} the electrode polarization caused by concentration difference, η_{ct} the electrode polarization caused by charge transfer, R_{AM} the polarization resistance of the active mass, R_{grid} the polarization resistance caused by the grid and $R_{\text{grid/AM}}$ the interface resistance between the grid and the active mass. The unit of the polarization resistance here should be expressed by $\Omega\,\text{cm}^2$.

Fig. 11 shows the polarization resistance distribution on automotive positive plate after different discharge times. Although the positive plate is discharged at 36 A, the polarization resistance is only about $1\,\Omega\,\text{cm}^2$ in the central part of the plate at the discharge time of 1 min (Fig. 11a), while the polarization resistance is near $2\,\Omega\,\text{cm}^2$ at the bottom and on the top. When the plate has been discharged for 4 min, the majority of polarization resistance is less than $2\,\Omega\,\text{cm}^2$. However, at this time, the polarization resistance rises to $2\text{–}4\,\Omega\,\text{cm}^2$ at the bottom and on the top (Fig. 11b). At the end of the discharge, the polarization resistance in the central part of the plate does not change very much, but it increases sharply at the bottom and on the top of the plate, especially on the top and far away from the lug. The polarization resistance reaches $4\text{–}10\,\Omega\,\text{cm}^2$ in different regions (Fig. 11c).

During the discharge of the automotive positive plate, what we are interested in is the change of the potential, U, in Eq. (2) or the polarization, $-\Delta U$, in Eq. (3). In our experiments, no real concentration polarization should be observed because the plate is only 12.5 cm high and the H_2SO_4 specific gravity only decreases by about $0.01\,\text{g cm}^{-3}$ during the discharge. Fig. 8 shows that the voltage drop up and down the plate is less than 30 mV at the 3 C discharge, which may be caused by the positive grid. Normally, the value of the voltage drop of the grid changes little during the discharge. So the change of the total polarization resistance in Fig. 11c is not chiefly brought about by the grid resistance, R_{grid}. Since the interface between the grid and the active mass is mainly formed during the curing, formation and the charge–discharge cycles, its resistance, $R_{\text{grid/AM}}$, changes little during one discharge period. The charge transfer polarization, η_{ct}, depends on the current density, which is low at the bottom and on the top of the plate in Figs. 4 and 6. Therefore, $\Delta\eta_{\text{ct}}$ should also have a low value and the very high overpotential in the bottom and top part of the plate must be attributed to the polarization resistance of the active mass R_{AM}. This R_{AM} reflects the active mass aggregation. The evolution of the polarization resistance in Fig. 11 is therefore mainly caused by the electrical connection between the particles of the active mass, too [21]. This non-uniform resistance on the positive plate should be closely related to its overcharge and its formation in the manufacturing process.

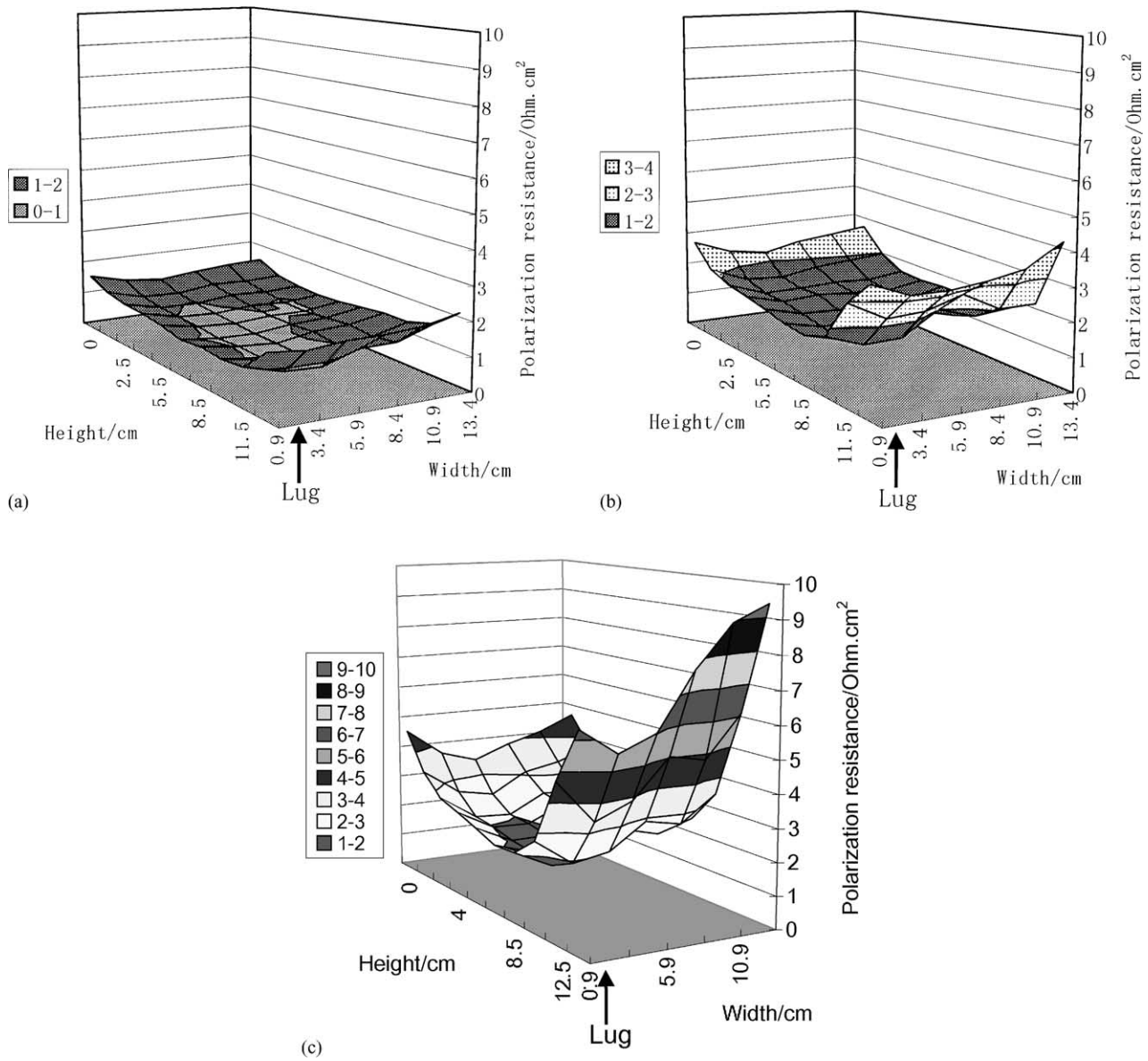

Fig. 11. The polarization resistance distribution on automotive positive plate during the discharge of 36 A. Discharge time: (a) 1 min; (b) 4 min; (c) 5.8 min.

3.5. Discharge of dry-charged positive plate

The performance of the dry-charged plate is very important to the automotive lead-acid battery. It normally depends on the positive plate if the negative plate is dried under the proper condition. The performance of the positive plate is closely related to the manufacture such as drying technology, the content of PbO_2 in the active mass and the soaking time and the temperature of the plate in the electrolyte before the use. We have measured the distributions of the current density and potential at the beginning, middle and end of the discharge after 20 min activated dry-charged plate. The results are similar to those obtained in Figs. 4–7, except for the overpotential. Fig. 12 shows the distribution of the positive potential at 36 A discharge when the dry-charged positive plate was immersed into the electrolyte for 20 min. For comparison, the data of the wet-charge plate are also given in Fig. 12. It is found that the positive potential of the dry-charged plate decreases by about 40 mV at the beginning of the discharge, as compared with the wet-charge plate. Since the electrolyte is superfluous in our experiments, it also improves the performance of the dry-charged plate to some extent. Therefore, the discharge time of the dry-charged plate is only about 30 s less than that of the wet-charge plate. But, in comparison with the wet-charge plate, its potential in the upper part of the plate decreases a little more slowly than that in the lower part of the plate. We also find that the homogeneity of dry-charged plates is poor and their discharge times are quite different, which is caused by the formation of the positive plate and its thermopassivation in the dry process [22,23].

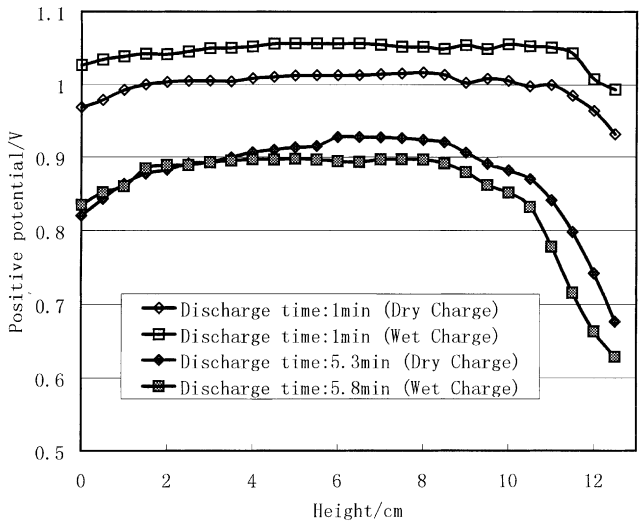

Fig. 12. The distribution of positive potential of the dry-charged and wet-charged plates during discharge of 36 A. Soaking time of the dry-charged plate: 20 min.

4. Conclusions

The resistance of the grid with the conventional orthogonal design increases with the extension of the distance away from the grid lug, but the resistance around the grid decreases because of the big frame.

At the beginning of the 3 C discharge, the distributions of the current density and potential are uniform on the automotive positive plate. As the positive plate is discharged, the polarization becomes increasingly higher at the bottom and on the top of the plate. At this time, quite non-uniform distribution of the current density appears on the positive plate. The current density at the bottom and on the top decreases sharply while it increases in the middle part because the total current on the plate does not change. If the polarization resistance is defined by the ratio of the polarization of the positive plate to the current density, the distribution of the polarization resistance can also be obtained during the discharge. In the early stage of the discharge, the distribution of the polarization resistance is uniform and only changes a little. Yet, the polarization resistance at the bottom and on the top increases greatly in the later stage of the discharge. The termination of the discharge is due to the polarization resistance evolution of the active mass at the bottom and on the top of the plate.

Although the automotive flooded positive plate is discharged at a high rate, the higher current density is observed in the lower part rather than in the upper part of the plate. It is different from the conventional viewpoint, which holds that the current density in the upper part should be higher than that in the lower part. This may be due to the improper formation of the positive plate, which may result in the differences of the electrical connection between active mass and the interface resistance between the grid and the active mass in different plate regions.

The performance of the dry-charged positive plate depends on its manufacturing processes. At the 3 C discharge, the polarization potential of the dry-charged plate increases by at least 40 mV in comparison with the wet-charged plate.

References

[1] S. Fouache, A. Chabrol, G. Fossati, M. Bassini, M.J. Sainz, L. Atkins, J. Power Sources 78 (1999) 12.
[2] M. Metikoš-Huković, R. Babić, S. Brinić, J. Power Sources 64 (1997) 13.
[3] L. Albert, A. Goguelin, E. Julliam, J. Power Sources 78 (1999) 12.
[4] P.T. Moseley, J. Power Sources 64 (1997) 47.
[5] M. Calábek, K. Micka, P. Bača, P. Křivák, J. Power Sources 85 (2000) 145.
[6] W.G. Sunu, B.W. Burrows, J. Electrochem. Soc. 129 (1982) 688.
[7] W.G. Sunu, B.W. Burrows, J. Electrochem. Soc 131 (1984) 1.
[8] L.E. Vaaler, E.W. Brooman, H.A. Fuggiti, J. Appl. Electrochem. 12 (1982) 721.
[9] T.C. Dayton, D.B. Edwards, J. Power Sources 85 (2000) 137.
[10] A.L. Ferreira, J. Power Sources 95 (2001) 255.
[11] D. Pavlov, S. Ruevski, J. Power Sources 95 (2001) 191.
[12] L. Narasimhan, P. Raj, Z. Hussain, J. Power Sources 78 (1999) 214.
[13] J.E. Manders, N. Bui, D.W.H. Lambert, J. Nararette, R.F. Neelson, E.M. Valeriote, J. Power Sources 73 (1998) 152.
[14] D. Pavlov, G. Papazov, J. Electrochem. Soc. 127 (1980) 2104.
[15] F.B. Diniz, L.E.P. Borges, B.B. Neto, J. Power Sources 109 (2002) 184.
[16] J.M. Stevenson, A.T. Kuhn, J. Power Sources 8 (1982) 385.
[17] E. Meissner, J. Power Sources 42 (1993) 103.
[18] J. Meiwes, H.-Ch. Skudeluy, J. Power Sources 27 (1989) 45.
[19] W.G. Sunu, B.W. Burrows, J. Electrochem. Soc. 128 (1981) 1405.
[20] Y. Guo, W. Li, L. Zhao, J. Power Sources 116 (2003) 193.
[21] E. Meissner, J. Power Sources 78 (1999) 99.
[22] D. Pavlov, St. Ruevski, J. Electrochem. Soc. 126 (1979) 1100.
[23] N. Anastasijevič, J. Garche, K. Wiesener, J. Power Sources 7 (1982) 201;
N. Anastasijevič, J. Garche, K. Wiesener, J. Power Sources 10 (1983) 43.